Steel and Composite Structures, *Vol. 35, No. 5 (2020) 701-715*
DOI: https://doi.org/10.12989/scs.2020.35.5.701

Perforated TWCF steel beam-columns: European design alternatives

Nadia Baldassino[1], Martina Bernardi*[1], Claudio Bernuzzi[2] and Marco Simoncelli[2]

[1]*Department of Civil, Environmental and Mechanical Engineering, Università di Trento, via Mesiano, 77, 38123, Trento, Italy*
[2]*Department of Architecture, Built Environment and Construction Engineering, Politecnico di Milano, piazza Leonardo da Vinci 32, 20133, Milano, Italy*

(*Received February 20, 2020, Revised May 14, 2020, Accepted May 15, 2020*)

Abstract. Steel storage racks are lightweight structures, made of thin-walled cold-formed members, whose behaviour is remarkably influenced by local, distortional and overall buckling phenomena, frequently mutually combined. In addition, the need of an easy and rapid erection and reconfiguration of the skeleton frame usually entails the presence of regular perforations along the length of the vertical elements (uprights). Holes and slots strongly influence their behaviour, whose prediction is however of paramount importance to guarantee an efficient design and a safe use of racks. This paper focuses on the behaviour of isolated uprights subjected to both axial load and bending moments, differing for the cross-section geometry and for the regular perforation systems. According to the European standards for routine design, four alternatives to evaluate the bending moment–axial load resisting domains are shortly discussed and critically compared in terms of member load carrying capacity.

Keywords: thin-walled members; storage racks; uprights; perforated beam-columns; design methods; M-N domains

1. Introduction

Thin-walled cold-formed (TWCF) steel members achieve their strength and stiffness through their complex shape. These engineered cross-sections guarantee high load carrying capacity with quite limited self-weight and, consequently, costs, making them very attractive for engineers (Fig. 1) (Dubina *et al.* 2013).

Due to the cold-forming processes, the thickness of TWCF members is generally not greater than 4mm and, for this reason, the profiles are sensitive to local, distortional and overall buckling phenomena (Dinis *et al.* 2014, Choi and Kwon 2018, Baldassino *et al.* 2019a). TWCF sections are frequently used in the logistic field, leading to quite complex structural systems which design requires specific engineering knowledge (Tilburgs 2013, Montuori *et al.* 2019). In these structures, the profiles adopted for the vertical elements (the so-called uprights) are generally characterised by open cross-section with a single axis of symmetry (Fig. 2). The non-coincidence between the shear centre and the cross-section centroid adds complexity to the prediction of the structural behaviour due to the high sensitivity to torsional effects. In addition, the need of a rapid erection of the rack and of the adjustment of the clear height of the bays to the pallet sizes, which could change over the time (Chen *et al.* 2019), requires the presence of regular perforation systems along the upright length (Fig. 2). It is worth noting that there is a great variability in both uprights cross-section geometries and type of perforations, that change from manufacturer to manufacturer (e.g. circular holes or elliptic and diamond slots), leading to the impossibility to define pure theoretical design approaches (El Kadi and Kiymaz 2015, Casafont *et al.* 2018). For the aforementioned reasons, the prediction of the load carrying capacity of uprights is really complex, as pointed out by the attention paid by researchers to this topic over the last 30 years (Sena Cardoso and Rasmussen 2016, Hancock 2016, El Kadi *et al.* 2017, Baldassino *et al.* 2019b).

Recently, great research efforts have been addressed to the development of design approaches accounting for the presence of perforations in columns and beam-columns (Moen 2008). At the moment, the 'design assisted by testing' approach (EN1990 2002, EN1993-1-3 2005, Baldassino and Zandonini 2011, Zandonini *et al.* 2014) is the strategy most commonly adopted in routine design, as suggested also by recent rack specifications (RMI 2008, EN15512 2009). The tests are essentially used to evaluate the ultimate resistance of a structural member or subassembly, under given load conditions, or to check the in-service behaviour of a structure (or a part of it). As well established, the upright design is usually based on the effective cross-section properties, i.e., the effective area (A_{eff}) and the effective section moduli (W_{eff}), that are always not greater than the associated gross properties (A_g and W_g). The assessment of the effective properties is based on the maximum load carrying capacity of the components, obtained through experimental tests (R_k), whose procedures

*Corresponding author, Ph.D. student
E-mail: martina.bernardi@unitn.it

http://www.techno-press.org/?journal=scs&subpage=8
ISSN: 1229-9367 (Print), 1598-6233 (Online)

Fig. 1 Structural applications of TWCF steel members (Metalsistem SpA)

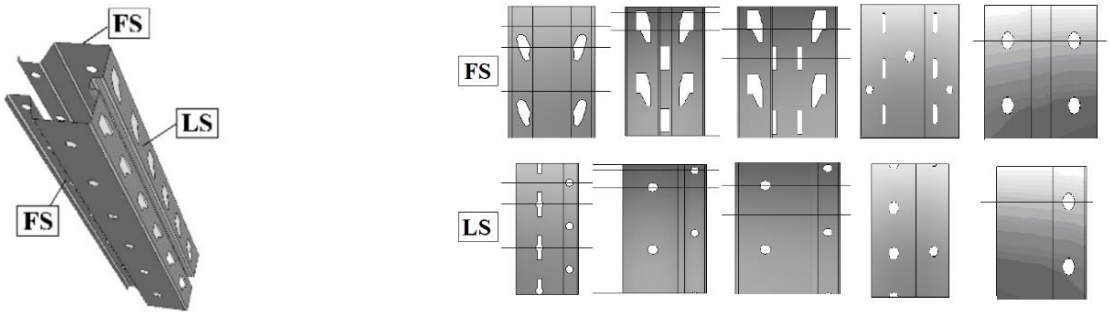

Fig. 2 Typical perforated TWCF members, lateral (LS) and frontal (FS) view

Table 1 Key tests recommended to assess the effective upright properties

	Stub-column test	Four points bending test
Section properties	Effective area $A_{eff} = \frac{R_k}{f_y}$ $Q^N = \frac{A_{eff}}{A_g}$	Effective section modulus $W_{eff} = \frac{R_k}{f_y}$ $Q^M = \frac{W_{eff}}{W_g}$
Test scheme (EN15512 2009, Baldassino *et al.* 2019c)		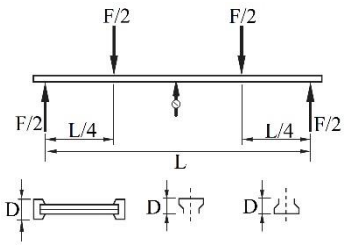

are accurately described in the Appendix A of the current EN15512 standard (EN15512 2009) and of the preliminary (pr) version of this standard (prEN15512 2018), which is currently subjected to public enquiry. Table 1 deals with the two key tests performed on the uprights in order to define the reduction factors Q^N and Q^M. Term Q is a factor representing the ratio between the gross and the effective quantities and apexes N and M refer to the axial and the bending moment loading condition, respectively. With reference to the current rack products, these factors are generally comprised between 0.7 and 1.0, where the unity is associated with the case of no reduction, i.e. the gross and effective cross-section parameters of interest are coincident.

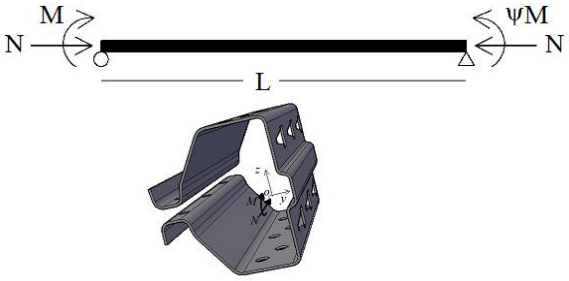

Fig. 3 Isolated member under axial load and gradient moment

In a rack structure, uprights are usually subjected to a combination of bending moments (M) and axial force (N). Therefore, their design requires a proper characterisation in presence of combined forces, leading to the definition of M-N resisting domains (Bernuzzi and Simoncelli 2015). Although the behaviour of TWCF sections subjected to combined axial load and bending moments has been experimentally investigated in the past (Torabian *et al.* 2015, Talebian *et al.* 2018), the experimental work on perforated storage rack uprights is quite limited (Bonada *et al.* 2016). As an alternative to a pure experimental approach, a mixed numerical-analytical approach combining FE results and standards formulations can be suitably adopted (Bernuzzi and Maxenti 2015). This approach, although promising, cannot be simply adopted for daily design practice. To deal with this drawback, a study focused on the evaluation of the M-N domains by using mixed experimental-analytical procedures has been performed. This topic is the core of the present paper. Five different perforated upright profiles with regular perforation systems have been studied and their load carrying capacity has been evaluated according to four different design alternatives. In the present paper, only the design approaches adopted in European standards have been considered and compared, although other design approaches, e.g. the DSM, are commonly used in other countries. The resisting axial load-bending moment domains have been defined and compared, considering the cases of isolated columns of practical interest for routine design. In the study, the method proposed by the prEN15512 (prEN15512 2018), which allows for taking into account directly for the presence of perforations, has been also considered. The advantage of this quite novel approach relies on the possibility to identify an 'equivalent' solid cross-section to include the influence of the perforations.

2. The considered cases

Rack design, as in traditional carpentry steel frames, is carried out in two subsequent steps:

- structural frame analysis to evaluate the set of the generalised forces in each structural component;
- safety checks, carried out on isolated members and joints.

In the paper, attention is addressed to isolated uprights with mono-symmetric cross-section subjected, at the member ends, to axial loads and bending moments about the section symmetry axis (*y* axis) (Fig. 3). This loading condition is representative of the rack response in the down-aisle direction, which is, in general, the most critical one for practical design purposes. In the study herein considered, reference is made to the following parameters:

- *the upright geometry*: five different cross-sections, conventionally named U, S, M, R and T, have been considered (Fig. 4), which have been previously tested in compression and in bending according to European standard code (EN15512 2009). Table 2 summarises the main properties of the cross-sections. In particular, the values of the squash load ($A_g \cdot f_y$) and the elastic bending moment ($W_{y,g} \cdot f_y$) are reported to allow for a general appraisal of the member performances. The area (A_g) and the section modulus ($W_{y,g}$) are referred to the gross cross-section and f_y is the nominal yielding strength (steel grade S350GD). Table 2 reports also the ratios between the second moments of area associated with the section principal axes ($I_{y,g}/I_{z,g}$), the uniform torsional and warping second moments of area ($I_{t,g}$ and $I_{w,g}$, respectively) and the y_s/t ratio, i.e. the distance between the shear centre and the centroid (y_s) over the thickness (t). No additional data are reported because of the confidentiality required by manufactures for their patented products herein considered. The differences in terms of perforation system can be appraised in Fig. 4, where the Q^N and Q^M values, evaluated on the basis of experimental results, are also reported;
- *the load condition*: a constant axial load is combined with a gradient bending moment expressed by means of the term ψ, i.e. the ratio between the minimum and the maximum end bending moment values (Fig. 3). Three ψ values have been considered: $\psi=1$ (uniform moment), $\psi=0$ (no moment at one end) and $\psi=-1$ (opposite moments at the two ends). At this aim, axial loads have been applied to the ends considering 13 different eccentricity values (e), evaluated with respect to the centroid of the gross cross-section, ranging from zero (column) to the infinite (beam);
- *the member slenderness*: reference has been made to three different values of the effective length of practical interest for routine design: $L=1m$, which is typical of

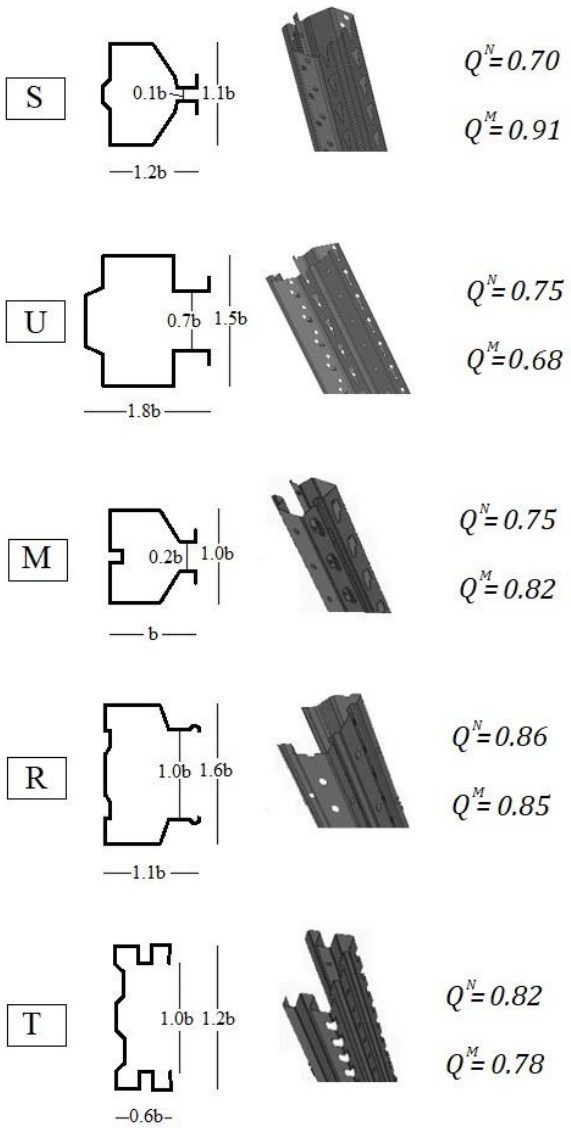

Fig. 4 Global view of the cross-sections considered in the study

Table 2 Key data of the considered uprights cross-sections

	S	U	M	R	T
$A_g \cdot f_y$ [kN]	182.83	260.87	205.55	357.38	239.27
$W_{y,g} \cdot f_y$ [kNm]	3.59	9.10	4.37	13.25	8.58
$I_{y,g}/I_{z,g}$	1.16	1.72	0.99	2.19	5.18
$I_{t,g}$ [mm^4]	306.5	408.1	619.0	2051.5	972.1
$I_{w,g}$ [mm^6]	$1.90 \cdot 10^9$	$4.9 \cdot 10^9$	$1.6 \cdot 10^9$	$5.6 \cdot 10^9$	$6.0 \cdot 10^8$
y_s/t	49.0	67.9	38.5	31.1	25.2

racks braced in the down-aisle direction, $L=2m$ and $L=3m$, which are generally associated to unbraced racks.

3. The equivalent cross-section

As expected and well-established, member perforations remarkably influence the uprights performance. Nevertheless, taking into account the effects of perforations is not an easy task, as already discussed in

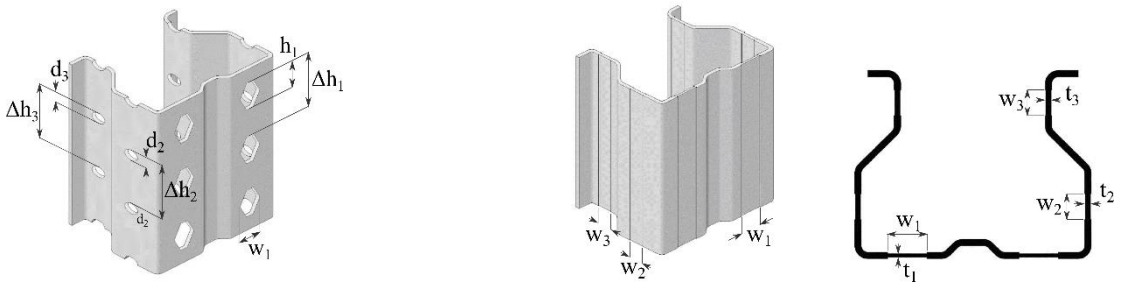

Fig. 5 The equivalent section, according to Annex G of prEN15512 (2018)

Table 3 Comparison of equivalent and gross geometric properties

Sections	A_{eq}/A_g	$I_{y,eq}/I_{y,g}$	$I_{z,eq}/I_{z,g}$	$I_{t,eq}/I_{t,g}$	$I_{w,eq}/I_{w,g}$
S	0.85	0.85	0.85	0.76	0.86
U	0.88	0.87	0.89	0.81	0.88
M	0.88	0.94	0.91	0.82	0.91
R	0.90	0.90	0.95	0.82	0.93
T	0.97	0.87	0.94	0.84	0.82

literature (Moen 2008, Casafont *et al.* 2013). A quite 'innovative' approach is included in the Annex G of the prEN15512 standard (prEN15512 2018), which accounts for regular perforations by locally reducing the profile thickness to obtain an equivalent solid cross-section, divided into strips of different thicknesses (Fig. 5). For a cross-section derived from a coil having a thickness of t, the equivalent thickness t_i of each strip containing one pattern of perforations is evaluated according to Eq. (1(a))

$$t_i = t\frac{\Delta h_i - h_i - \xi_i w_i}{\Delta h_i} \qquad i = 1,..., N \tag{1a}$$

where w_i and h_i are the width and the height of the perforations (conveniently substituted by d_i in case of circular perforations) and Δh_i represents the distance between the regular perforations along the cross-section. Term ξ_i is a suitable influence factor defined as

$$\xi_i = \frac{\Delta h_i - h_i}{2w_i} \le 1.5 \tag{1b}$$

Once defined the equivalent cross-section, all the geometric properties can be evaluated according to well-established procedures, i.e., the use of appropriate software or by applying the calculation methods given, for example, in EN 1993-1-3 (EN1993-1-3 2005).

Table 3 presents, for the uprights considered in this study, the ratios between the equivalent geometric properties (pedix *eq*) obtained by applying Eqs. (1) and the gross (pedix *g*) ones.

The values reported in the table stress out the importance of the perforations system. In particular, the area and second moments of area ratios have differences up to 15%, while the influence on the torsional parameters is more severe and up to 24%. It is worth noting that the introduction of the equivalent section is the first attempt provided by the European standards to take analytically into account the influence of the perforations. The work described in this paper provides a first attempt of application of this approach on the uprights design.

4. The EU design procedure

As mentioned before, four different European design procedures have been considered in the study. Specifically, reference is made to the design procedures addressed in:

- EN15512 (EN15512 2009) which is the standard addressed to the steel storage racks static design;
- part 1-3 of Eurocode 3 (EN1993-1-3 2005);
- part 1-1 of Eurocode 3, specifically the General Method (GEM) (EN1993-1-1 2005);
- prEN version of EN15512 (prEN15512 2018), that also coincides with the approach proposed in the final draft of EN1993-1-3 document (EN1993-1-3 2018).

In the following, these four approaches are shortly introduced and applied to the considered uprights.

4.1 Verification in accordance with EN15512

The European design of steel storage pallet systems is usually carried out on the basis of the EN15512 (EN15512 2009), which is addressed to static design of pallet racking systems. In particular, for beam-columns, when the lateral-torsional buckling is taken into account, the following condition has to be fulfilled

$$\left(\frac{N_{Ed}}{\frac{\chi_{\min} A_{eff} f_y}{\gamma_M}}\right)+\left(k_{LT}\frac{M_{y,Ed}}{\frac{\chi_{LT} W_{eff,y} f_y}{\gamma_M}}\right)=\left(\frac{N_{Ed}}{N_{b,Rd}}\right)+\left(\frac{M_{y,Ed}}{M_{b,Rd}}\right)\le 1 \quad (2)$$

in which χ is the reduction factor accounting for the buckling phenomena (flexural, torsional or flexural-torsional) as explained in the following, f_y is the material yielding strength, A_{eff} and $W_{eff,y}$ are, the effective area and the effective cross-section modulus about the principal cross-section symmetry axis (y axis) of the section, respectively, and γ_M is the material safety factor.

Referring to the reduction factors, χ_{min} is the smallest of the reduction factors accounting for global and distortional buckling modes. While the former can be theoretically evaluated, the latter can be appraised only via experimental tests (as stated in the code). The suitable reduction factor χ is defined as

$$\chi=\frac{1}{\varphi+\sqrt{\varphi^2-\bar{\lambda}^2}}\le 1 \quad (3)$$

where

$$\varphi=0.5\left[1+\alpha\left(\bar{\lambda}-0.2\right)+\bar{\lambda}^2\right] \quad (4)$$

The imperfection factor α depends on the buckling curve selected on the basis of the type of cold-formed section and on the buckling axis. The relative slenderness for an element in pure compression $\bar{\lambda}$ is defined as

$$\bar{\lambda}=\sqrt{\frac{A_{eff} f_y}{N_{cr}}} \quad (5)$$

in which N_{cr} is the elastic critical load of the gross cross-section for the appropriate buckling mode that can be determined via suitable theoretical approaches (Dubina *et al.* 2013), as shown in Appendix A.

As to the bending moment contribution (second term in Eq. (2)), the reduction factor for lateral-torsional buckling χ_{LT} is determined as defined in Eq. (3) by substituting coefficients φ and α with φ_{LT} and α_{LT}, respectively. Furthermore, the relative slenderness for axial load ($\bar{\lambda}$) in Eqs. (3) and (4) has to be replaced by the one for the lateral-torsional bending buckling ($\bar{\lambda}_{LT}$), defined as

$$\bar{\lambda}_{LT}=\sqrt{\frac{W_{eff,y} f_y}{M_{cr,B}}} \quad (6)$$

where the term $M_{cr,B}$ is the elastic critical moment of the gross cross-section for lateral-torsional buckling that can be determined via theoretical approaches (Dubina *et al.* 2013), as reported in Appendix A.

Term k_{LT} of Eq. (2) is given by the expression

$$k_{LT}=1-\frac{\mu_{LT} N_{Ed}}{\chi_z A_{eff} f_y}\le 1 \quad (7)$$

with

$$\mu_{LT}=0.15\left(\bar{\lambda}_z \beta_{M,LT}-1\right)\le 0.9 \quad (8)$$

where ($\bar{\lambda}_z$) is the relative slenderness for flexural buckling about the z axis (principal non-symmetry axis) in accordance with Eq. (5), and $\beta_{M,LT}$ is an equivalent uniform moment factor for lateral-torsional buckling, accounting for the bending moment distribution between two subsequent braced points. If reference is made to the loading case reported in Fig. 3, where ψ is the ratio between minimum and maximum end bending moment values ranging between *-1* and *1*, $\beta_{M,LT}$ is given by the expression

$$\beta_{M,LT}=1.8-0.7\psi \quad (9)$$

It should be noted that this design approach was already proposed in the previous version of Eurocode 3 (ENV1993-1-1 1992) but it was removed from the EN versions (EN1993-1-1 2005) due to its inaccuracy, not only for members having mono-symmetric cross-section, but, in several cases, also for bi-symmetric beam-column cross-sections. Furthermore, no practical indications are given to designers for what concerns the elastic buckling interaction between axial force and bending moment.

4.2 Verification in accordance with EN1993-1-3

As an alternative, reference can be made to the European standard for the design of cold-formed members, i.e., Eurocode 3 part 1-3 (EN1993-1-3 2005). Upright verification check is satisfied when

$$\left(\frac{N_{Ed}}{N_{b,Rd}}\right)^{0.8}+\left(\frac{M_{y,Ed}}{M_{b,Rd}}\right)^{0.8}\le 1 \quad (10)$$

where $N_{b,Rd}$ is the column design buckling resistance (for flexural, torsional or torsional-flexural buckling) and $M_{b,Rd}$ is the beam design bending moment resistance, accounting for lateral-torsional buckling. Owing to the absence of specific rules to evaluate the effective cross-section properties of perforated members, both $N_{b,Rd}$ and $M_{b,Rd}$ have been evaluated as reported in the previous sub-section.

If the design approaches proposed by EN15512 and EN1993-1-3 are compared, it can be observed that the only differences between Eq. (10) and Eq. (2) rely in the presence of the exponents 0.8 and the absence of term k_{LT} in the bending moment contribution.

4.3 Verification in accordance with EN1993-1-1

For the stability checks of structural components having geometrical, loading and/or supporting irregularities, Eurocode 3 in its part 1-1 proposes a quite innovative design approach, that is the so-called *general method* (GEM) (EN1993-1-1 2005). Uprights sections can be considered a typical example of these not-standard structural components, being characterised by mono-symmetric cross-sections as well as by the presence of perforations.

According to the general method, overall out-of-plane buckling resistance is verified when

$$\frac{\chi_{op}\alpha_{ult,k}}{\gamma_M} \geq 1 \tag{11}$$

where $\alpha_{ult,k}$ is the minimum load multiplier evaluated with reference to the cross-section resistance taking into account its in plane behaviour without considering lateral or lateral-torsional buckling, χ_{op} is the buckling reduction factor referred to the overall structural system accounting for lateral or lateral-torsional buckling and γ_M is the material safety factor.

The buckling reduction factor χ_{op} should be evaluated on the basis of relative frame slenderness $\overline{\lambda}_{op}$ of the structural component, which is defined as

$$\overline{\lambda_{op}} = \sqrt{\frac{\alpha_{ult,k}}{\alpha_{cr,op}}} \tag{12}$$

where $\alpha_{cr,op}$ is the minimum buckling multiplier, considering the lateral or lateral-torsional buckling and without accounting for in-plane flexural buckling.

The reduction factor χ_{op} can be taken equal to the minimum value between the one for lateral buckling (χ) and the one for lateral-torsional buckling (χ_{LT}) appraised according to Eq. (3), considering the global relative slenderness $\overline{\lambda}_{op}$.

The ultimate load multiplier for resistance, $\alpha_{ult,k}$, is appraised as

$$\frac{1}{\alpha_{ult,k}} = \frac{N_{Ed}}{N_{Rk}} + \frac{M_{y,Ed}}{M_{y,Rk}} \tag{13}$$

where N_{Rk} and $M_{y,Rk}$ are the squash load and the first yielding moment, respectively, of the effective cross-section, as recommended by Eurocode 3.

By combining Eqs. (11) and (13), it results

$$\frac{\frac{N_{Ed}}{N_{Rk}}}{\gamma_M} + \frac{\frac{M_{y,Ed}}{M_{y,Rk}}}{\gamma_M} \leq \chi_{op} \tag{14}$$

Eurocode 3 part 1-1 suggests a FE approach for the evaluation of $\alpha_{cr,op}$ which is not a viable strategy for the daily design practice. In the present study, it has been assumed that

$$\frac{1}{\alpha_{cr,op}} = \frac{N_{Ed}}{N_{cr}} + \frac{M_{y,Ed}}{M_{cr,B}} \tag{15a}$$

that could be written also as

$$\alpha_{cr,op} = \frac{N_{cr}M_{cr,B}}{N_{Ed}M_{cr,B} + N_{cr}M_{y,Ed}} \tag{15b}$$

where N_{cr} and $M_{cr,B}$ are the elastic critical load and the beam elastic critical moment, respectively, whose relationships are reported in Appendix A. Furthermore, for their evaluation the equivalent cross-section defined in section 3 has been considered.

4.4 Verification in accordance with prEN15512

In this study, the prEN15512 (prEN15512 2018) standard has been also considered. It is worth noting that the prEN15512 approach is analogous to the one proposed in the first draft of the Eurocode 3 part 1-3 (EN1993-1-3 2018), with the only difference that prEN15512 requires the use of the equivalent section introduced in section 3.

The following interaction formula, reduced for the case of beam-columns subjected solely to one bending moment (i.e., $M_{y,Ed}$), are proposed:

$$\left(C_{x,y}\frac{N_{Ed}}{\chi_y N_{Rd}}\right)^{A_y} + \frac{M_{y,Ed}}{M_{y,Rd}} \leq 1 \tag{16a}$$

$$\left(C_{x,z}\frac{N_{Ed}}{\chi_z N_{Rd}}\right)^{A_z} + \left(C_{x,LT}\frac{M_{y,Ed}}{\chi_{LT} M_{y,Rd}}\right)^{B_z} \leq 1 \tag{16b}$$

where the reduction factors χ can be evaluated via Eq. (3) by considering the equivalent cross-section (§3).

Terms N_{Rd} and $M_{y,Rd}$ are the squash load and the first yielding moment, respectively, evaluated considering the effective section properties. The exponents A and B depend on the reduction factors χ (Eq. (3)) and on the ratios μ_y or μ_z given by expressions

$$\mu_y = \frac{\frac{M_{y,Rd}}{W_{el,y} f_y}}{\gamma_M} \geq 1 \tag{17a}$$

$$\mu_z = \frac{\frac{M_{z,Rd}}{W_{el,z} f_y}}{\gamma_M} \geq 1 \tag{17b}$$

It is worth noting that the Code does not provide details about the evaluation of W_{el} and, as a consequence, the Authors decided to use W_{el} of the equivalent section.

The interaction factors $C_{x,y}$ and $C_{x,LT}$, accounting for the variation of the moments along the member, for a specific cross-section location along the member, are defined as follows

$$C_{x,y} = \chi_y + (1-\chi_y)\sin\left(\frac{\pi x_s}{L_{cr,y}}\right) \tag{18}$$

and

$$C_{x,LT} = \chi_{LT} + (1-\chi_{LT})\sin\left(\frac{\pi x_s}{L_{cr,LT}}\right) \tag{19}$$

where $L_{cr,y}$ and $L_{cr,LT}$ are the buckling lengths for the relevant buckling mode, while x_s defines the position of the cross-section under consideration. In the analyses herein presented, $x_s=L/2$ has been considered.

5. Resisting domains

For each of the previous discussed methods and for each

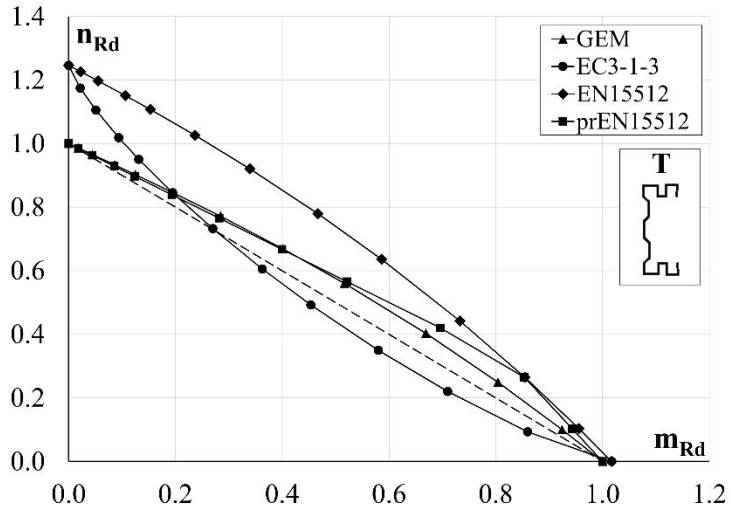

Fig. 6 m_{Rd}-n_{Rd} domains for the T section

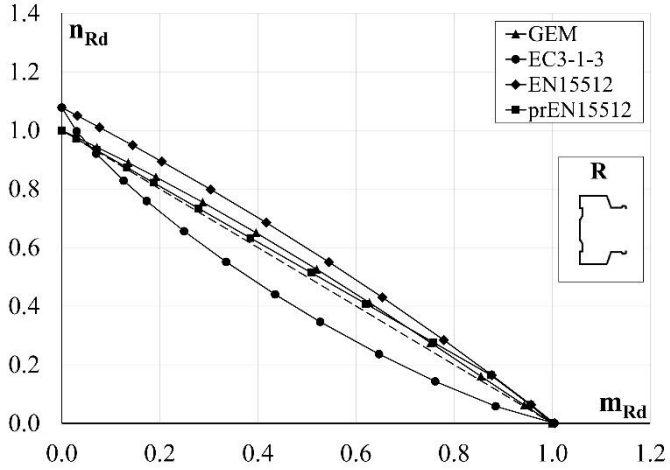

Fig. 7 m_{Rd}-n_{Rd} domains for the R section

of the five considered cross-sections, the resisting beam-column domain has been evaluated by imposing the unity as final result of the verification check equation, i.e., the design load corresponding to the load carrying capacity has been determinated. Typical domains are reported in Fig. 6, which is related, as an example, to the T cross-section (Table 2, Fig. 3) with a length of *2 m* and a bending distribution parameter ψ=*-1*. The domains are proposed in the non-dimensional m_{Rd}-n_{Rd} form: m_{Rd} is the ratio between the bending resistance over the pure bending resistance based on the equivalent cross-section used to evaluate the lateral buckling load. Similarly, n_{Rd} has been obtained dividing the axial resistance by the pure axial resistance evaluated by considering the critical buckling load associated with the equivalent cross-section. In the same figure, the linear domain is presented too, by means of a dashed line. It is worth noting that, in Figs. 6-10 the n_{Rd} related to both the EN1993-1-3 and EN15512 approaches are greater than 1.0 due to the use of the equivalent cross-section to evaluate the non-dimensional terms.

A similar trend of the domains has been observed also for the other considered sections, as it appears in Figs. 7-10. To limit the length of the paper, only the domains related to the load condition ψ=*-1* and to the member length of *2m* have been reported in these figures that are however representative for all the other cases.

It can be noted that, considering the case of pure axial load and pure bending moment, the EN15512 and the EN1993-1-3 approaches give the same values, that are slightly higher than the ones obtained with the other two approaches. This is due to the different section properties considered to evaluate the buckling loads (i.e., effective cross-section vs. gross cross-section). Independently of the profile, the EN15512 domain is always represented by a straight line while the EN1993-1-3 one always presents a concavity, with values lower than the ones associated with the EN15512. The GEM approach is influenced by the profile shape, resulting in a quite linear or a strongly non-linear domain, as in case of R- and M-upright, respectively.

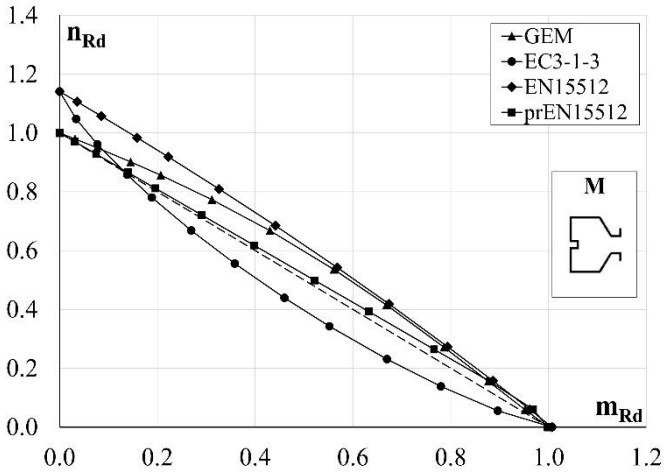

Fig. 8 m_{Rd}-n_{Rd} domains for the M section

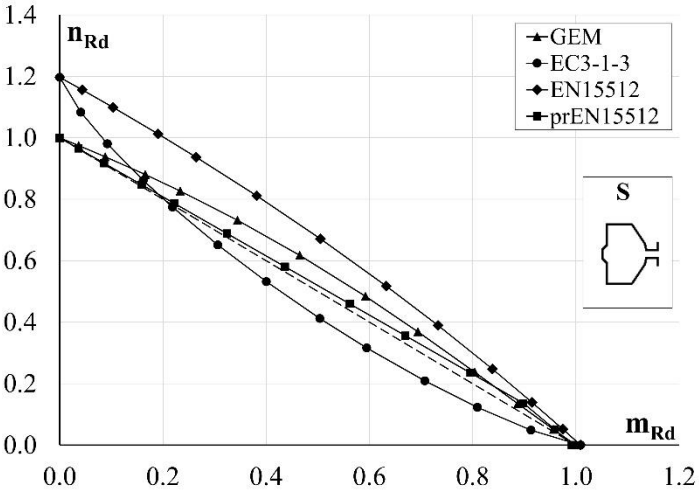

Fig. 9 m_{Rd}-n_{Rd} domains for the S section

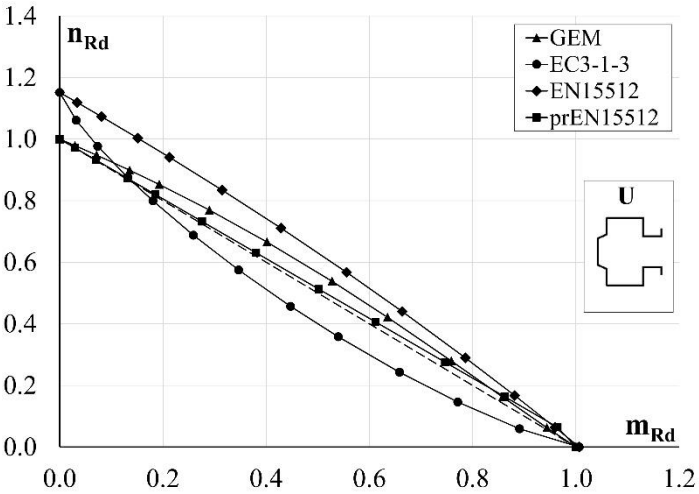

Fig. 10 m_{Rd}-n_{Rd} domains for the U section

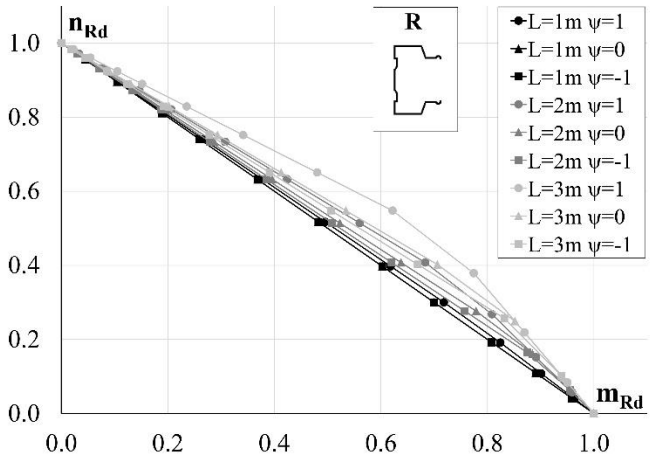

Fig. 11 m_{Rd}-n_{Rd} domains for the R section, according to prEN15512 (prEN15512 2018) approach

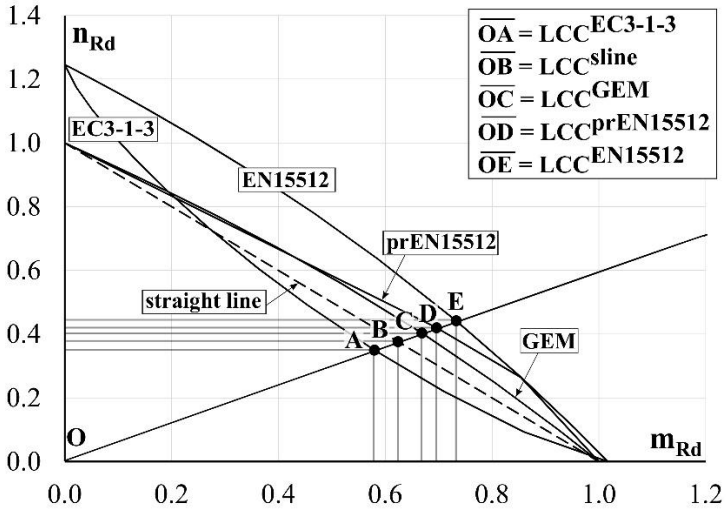

Fig. 12 m_{Rd}-n_{Rd} domains and LCC^L definition

Focusing attention on the prEN15512 method, which is of great interest for designers, it can be noted that the associated domains are always convex. Fig. 11 presents, as an example, the domains for all the considered cases associated with the R cross-section: increasing the length of the upright, the convexity increases, too. The curves associated with $\psi=-1$ and $\psi=0$ are practically coincident, slightly different from the ones associated with $\psi=1$, owing to the more severe condition with respect to the compressed part of the member.

In order to compare the outcomes of the considered approaches, for each *L-th* design procedure, the Load Carrying Capacity index (LCC^L) has been introduced. LCC^L is defined as shown in Fig. 12 and evaluated as

$$LCC^L = \sqrt{\left(m_{Rd}^L\right)^2 + \left(n_{Rd}^L\right)^2} \tag{20}$$

To compare the different approaches, reference has been made to the LCC^{sline} that is the value associated with the simplified linear domain (dashed lines in Figs. 6-10). The LCC^L/LCC^{sline} ratios are shown in Fig. 13.

In the figure, all the results are presented by distinguishing only the length values, i.e., different cross-sections and load conditions have been grouped together. The figure is divided in four quadrants:

- quadrant A, which compares the GEM and the EC3-1-3 approaches;
- quadrant B, which compares the EN15512 and the EC3-1-3 approaches;
- quadrant C, which compares the EN15512 and the prEN15512 approaches;
- quadrant D, which compares the GEM and the prEN15512 approaches.

In each quadrant, the vertical and horizontal straight lines in correspondence of unity allow identifying how the domain associated with the considered method is close to the linear one, i.e. the closer the markers to the unity line and the closer the LCC^L to the LCC^{sline}. In particular, it can be noted that:

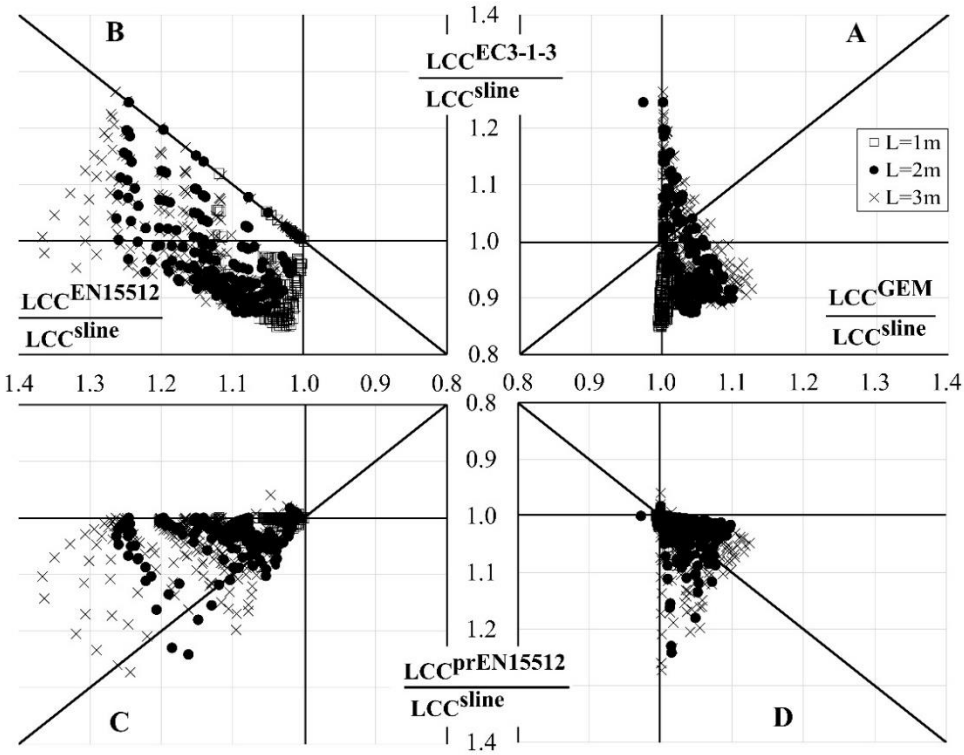

Fig. 13 Comparison between all the EU design approaches

- the markers associated with the GEM domains are in the range 0.99-1.12 showing that the related load carrying capacities are higher but close to the ones associated with the linear domains;
- both the EN15512 and prEN15512 approaches lead to LCC^{L}/LCC^{sline} ratios higher than the unity. In details, the $LCC^{EN15512}/LCC^{sline}$ and the $LCC^{prEN15512}/LCC^{sline}$ ratios are up to 1.37 and 1.27, respectively;
- unlike the previous approaches, in several cases the EC3-1-3 one is more severe than the linear approximation, in fact, the most of the markers are in the range 0.85-1.

A direct comparison between the different methods can be performed by considering the bisector lines in Fig. 13: being the cross-section, the length of profiles and the loading case the same, the two methods give the same output when the related marker is on the bisector line. In addition, each sub-domain defined by the bisector line allows to identify the method which provides higher values in terms of load carrying capacity. The comparison between the methods shows that:

- GEM vs. EC3-1-3 methods (quadrant A): the application of GEM leads, in general, to load carrying capacity values greater than the ones of the EC3-1-3. When the length of the profiles increases ($L=3$ *m*) a clear trend can not be identified;
- EN15512 vs. EC3-1-3 methods (quadrant B): the EN15512 load carrying capacity values are greater that the EC3-1-3 ones and, in few cases, the methods lead to the same results;
- EN15512 vs. prEN15512 methods (quadrant C): in the most of the considered cases (89%) the prEN15512 method results more conservative than the EN15512 one;
- GEM vs. prEN15512 methods (quadrant D): a clear trend can not be identified, although, for the shortest length (1 m), the prEN15512 leads to higher load carrying capacity values than the GEM.

As a general conclusion, it can be noted that the differences between the considered design alternatives are not negligible for practical design purposes: greater than 30%. From an engineering point of view, the application of one approach rather than another strongly affects the design output, reflecting in considerably different weights and costs of the storage system.

To get an appraisal about the effect of the selection of one method rather than another, Fig. 14 presents, for each *L-th* method, the ratios between LCC^{L} and the minimum *LCC* appraised amongst the four design alternatives (LCC^{min}). It can be noted that differences between the performances predicted by the four different methods are non-negligible and are up to 40%. In detail, it is worth noting that, frequently, the EN 1993-1-3 method is the most conservative, while the most 'generous' ones are the EN15512 and the prEN15512. As an example, if the value of 1.15 is considered, it can be noted that it is exceeded by 62% of $LCC^{EN15512}/LCC^{min}$ ratios and by 24% of $LCC^{prEN15512}/LCC^{min}$ ratios while decrease up to 6% and 18% for $LCC^{EC3\text{-}1\text{-}3}/LCC^{min}$ and LCC^{GEM}/LCC^{min}, respectively.

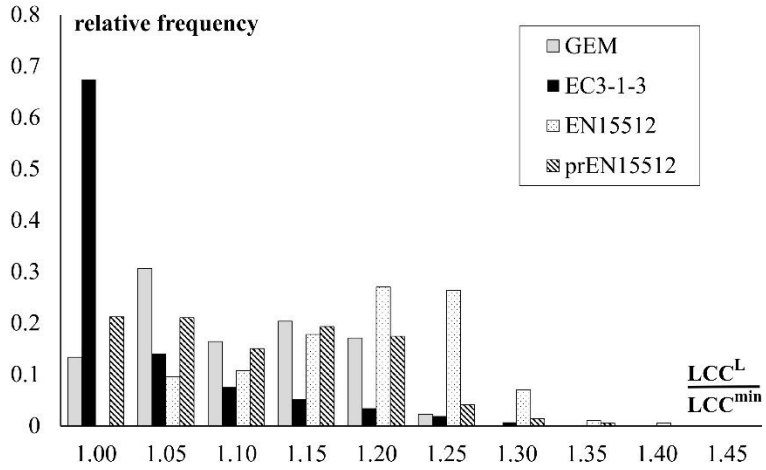

Fig. 14 Frequency distribution of LCC^{L}/LCC^{min} ratio considering all the cases

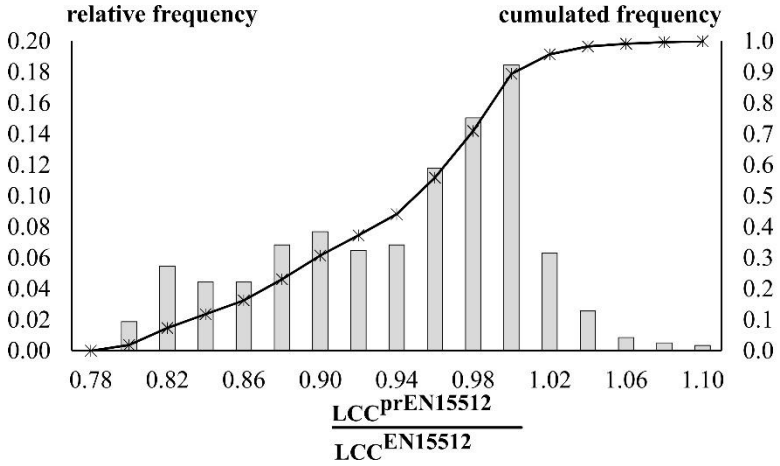

Fig. 15 Frequency distribution of $LCC^{prEN15512}/LCC^{EN15512}$ ratio grouping all the cases

Finally, focusing on the differences between the new and the current approach recommended in the EU rack design codes, Fig. 15 presents the distribution of the $LCC^{prEN15512}/LCC^{EN15512}$ ratio. It can be noted that, independently of the cross-section type, the results are mainly lower than unity, therefore the prEN15512 method is, in general, more conservative than the EN15512 one. Differences are higher in the case of slender beam-columns ($L=3m$), especially with $\psi=-1$, and they became lower than 8% in case of $L=1$ *m* with constant bending distribution, i.e., $\psi=1$.

6. Conclusions

The behaviour of rack uprights, that are usually cold-formed thin-walled profiles, is quite complex to predict because of the interactions between different forms of instability and the presence of perforations. Safety reasons and economical aspects stress the need of an optimized design of these elements which result in complex cross-section geometries further increasing the design difficulties.

The design procedures usually adopted for these kind of profiles are based on the so-called 'design by testing', which combines experimental results and analytical equations. In case of axial force and bending moment acting on the member, as for the rack uprights, the design should properly take into account the interaction between the generalised forces. A viable approach seems represented by the determination of the M-N resisting domains, that is the issue investigated in the paper.

Four different European design alternatives have been considered and, accordingly, the M-N domains have been determined and compared for a set of cases of practical interest for design purposes. In details, five perforated rack uprights with different cross-section have been considered, analyzing three different length values and three bending moment distributions. The M-N domains have been obtained by applying eccentric axial forces with eccentricities ranging from *0* (pure axial force) to infinite (pure bending moment).

From the discussed research outcomes, it can be pointed out that:

- the prEN15512 is the only standard which explicitly takes into account the presence of perforations through the introduction of an equivalent cross-section. For the considered cases, the use of the equivalent section leads to a reduction of the geometrical properties of the gross section up to 24%;
- the non-dimensional resisting domains (m_{Rd}-n_{Rd}) associated to the considered methods differ for both the shape and the load carrying capacity with differences up to 40%;
- the approach proposed by the prEN15512 is more conservative than the one proposed in the EN15512: differences are up to 20%;
- the general trend of the non-dimensional domains is quite independent on the bending moment distribution (ψ value) and on the cross-section shape.

As a general comment, it can be remarked that the EU standards investigated in this paper prescribe quite different design approaches for beam-column which are not always clearly detailed. This could lead to design assumptions reflecting, as demonstrated by the discussed data, in different values of the load carrying capacity. Finally, it is worth noting that, in the framework of this study, tests on full scale unbraced racks have been planned (Gelmini and di Gioia 2017) in order to allow for a more accurate appraisal of the safety associated with these considered methods.

References

Baldassino, N., Bernuzzi, C. and Simoncelli, M. (2019a), "Evaluation of European approaches applies to design of TWCF steel members", *Thin-Wall. Struct.*, **143**, 106-186. https://doi.org/10.1016/j.tws.2019.106186.

Baldassino, N., Bernuzzi, C. and Simoncelli, M. (2019b), "Experimental vs. theoretical design approaches for thin-walled cold-formed steel beam-columns", *Adv. Steel Constr.*, **15**(1), 55-65. https://doi.org/10.18057/IJASC.2019.15.1.8.

Baldassino, N., Bernuzzi, C., di Gioia, A. and Simoncelli, M. (2019c), "An experimental investigation on solid and perforated steel storage racks uprights", *J. Constr. Steel Res.,* **155**, 409-425. https://doi.org/10.1016/j.jcsr.2019.01.008.

Baldassino, N. and Zandonini, R. (2011), "Design by testing of industrial racks", *Adv. Steel Constr.*, **7**(1), 27-47. https://doi.org/10.18057/IJASC.2011.7.1.3.

Bernuzzi, C. and Maxenti, F. (2015), "European alternatives to design perforated thin-walled cold-formed beam-columns for storage steel systems", *J. Constr. Steel Res.*, **110**, 121-136. https://doi.org/10.1016/j.jcsr.2015.02.021.

Bernuzzi, C. and Simoncelli, M. (2015), "European design approaches for isolated cold-formed thin-walled beam–columns with mono-symmetric cross-section", *Eng. Struct.*, **86**, 225-241. https://doi.org/10.1016/j.engstruct.2014.12.040.

Boissonnade, N., Greiner, R., Jaspart, J.P. and Lindner, J. (2006), *Rules for Member Stability in EN 1993-1-1 Background Documentation and Design Guidelines*, Publication No. 119, ECCS European Convention for Structural Steelworks, Brussels, Belgium.

Bonada, J., Pastor, M.M., Roure, F. and Casafont, M. (2016), "Distortional influence of pallet rack uprights subject to combined compression and bending", *Structures*, **8**, 275-285. https://doi.org/10.1016/j.istruc.2016.05.007.

Casafont, M., Bonada, J., Pastor, M.M., Roure, F. and Susín, A. (2018), "Linear buckling analysis of perforated cold-formed steel storage rack columns by means of the Generalised Beam Theory", *Int. J. Struct. Stab. Dynam.*, **18**(1), 1850004. https://doi.org/10.1142/S0219455418500049.

Casafont, M., Pastor, M.M., Roure, F., Bonada, J. and Peköz, T. (2013), "Design of steel storage rack columns via the Direct Strength Method", *J. Struct. Eng.*, **139**(5), 669-679. https://doi.org/10.1061/(ASCE)ST.1943-541X.0000620.

Choi, J.Y. and Kwon, Y.B. (2018). "Direct strength method for high strength steel welded section columns", *Steel Compos. Struct.*, **29**(4), 509-526. https://doi.org/10.12989/scs.2018.29.4.509.

Chen, C., Shi, L., Shariati, M., Toghroli, A., Mohamad, E.T., Bui, D.T. and Khorami, M. (2019), "Behavior of steel storage pallet racking connection – A review", *Steel Compos. Struct.*, **30**(5), 457-469. https://doi.org/10.12989/scs.2019.30.5.457.

Dinis, P.B., Young, B. and Camotin, D. (2014), "Local-distortional interaction in cold-formed steel rack-section column", *Thin-Wall. Struct.*, **81**, 185-195. https://doi.org/10.1016/j.tws.2013.09.010.

Dubina, D., Ungureanu, V. and Landolfo, R. (2013), *Design of Cold-Formed Steel Structures. Eurocode 3: Design of Steel Structures-Part 1-3 Design of Cold-Formed Steel Structures*, ECCS European Convention for Structural Steelworks, Brussels, Belgium, and Wilhelm Ernst & Sohn, Berlin, Germany.

El Kadi, B., Cosgun, C., Mangir, A. and Kiymaz, G. (2017). "Strength upgrading of steel storage rack frames in the down-aisle direction", *Steel Compos. Struct.*, **23**(2), 143-152. https://doi.org/10.12989/scs.2017.23.2.143.

El Kadi, B. and Kiymaz, G. (2015). "Behavior and design of perforated steel storage rack columns under axial compression", *Steel Compos. Struct.*, **18**(5), 1259-1277. https://doi.org/10.12989/scs.2015.18.5.1259.

EN1990 (2002), Eurocode – Basis of structural design, European committee for Standardization, Brussels, Belgium.

EN1993-1-1 (2005), Eurocode 3 - Design of steel structures - Part-1-1: General rules and rules for buildings, European committee for Standardization, Brussels, Belgium.

EN1993-1-3 (2005), Eurocode 3 - Design of steel structures - Part-1-3: General rules: supplementary rules for cold-formed members and sheeting, European committee for Standardization, Brussels, Belgium.

EN1993-1-3 first draft new (2018), Eurocode 3 - Design of steel structures - Part-1-3: General rules: supplementary rules for cold-formed members and sheeting, European committee for Standardization, Brussels, Belgium.

EN15512 (2009), Steel storage systems - Adjustable pallet racking systems - Principle for structural design, European committee for Standardization, Brussels, Belgium.

ENV1993-1-1 (1992), Eurocode 3 - Design of steel structures - Part-1-1: General rules and rules for buildings, European committee for Standardization, Brussels, Belgium.

Gelmini, L. and di Gioia, A. (2017), "La torre prove della divisione ricerca e sviluppo di Metalsistem S.p.A. – The test tower of Metalsistem S.p.A. R&D Division", *Costruzioni Metalliche*, **6**, 71-77.

Hancock, G.J. (2016), "Cold-formed structures: Research review 2013-2014", *Advanced in Structural Engineering*, **961**, 1-43. https://doi.org/10.1177/1369433216630145.

Moen, C.D. (2008), "Direct Strength design of cold-formed steel members with perforations", Ph.D. Dissertation, Johns Hopkins University, Baltimore, Maryland.

Montuori, R., Gabbianelli, G., Nastri, E. and Simoncelli, M. (2019), "Rigid plastic analysis for the seismic performance evaluation of steel storage racks", *Steel Compos. Struct.*, **32**(1), 1-19. https://doi.org/10.12989/scs.2019.32.1.001.

prEN15512 (2018), Steel storage systems - Adjustable pallet

racking systems - Principle for structural design, European committee for Standardization, Brussels, Belgium.
RMI (2008), Specification for the design, testing and utilization of industrial steel storage racks, Racking Manufacturers Institute, Charlotte, NC, USA.
Sena Cardoso, F. and Rasmussen, K.J.R. (2016), "Finite element (FE) modelling of storage rack frames", *J. Constr. Steel Res*., **126**, 1-14. https://doi.org/10.1016/j.jcsr.2016.06.015.
Talebian, N., Gilbert, B.P., Pham, C.H., Chariere, R. and Karampour, H. (2018), "Local and distortional biaxial bending capacities of cold-formed steel storage rack uprights", *Journal of Structural Engineering (ASCE)*, **144**(6): 04018062. https://doi.org/10.1061/(ASCE)ST.1943-541X.0002029.
Tilburgs, K. (2013), "Those peculiar structures in cold-formed steel: 'racking and shelving'", *Steel Constr*., **6**(2), 95-106. https://doi.org/10.1002/stco.201310016.
Torabian, S., Zheng, B. and Schafer, B.W. (2015), "Experimental response of cold-formed steel lipped channel beam-columns", *Thin-Wall. Struct*., **89**, 152-168. https://doi.org/10.1016/j.tws.2014.12.003.
Zandonini, R., Baldassino, N. and Freddi, F. (2014), "Robustness of steel-concrete flooring systems – An experimental assessment", *Stahlbau*, **83**(9), 608-613. https://doi.org/10.1002/stab.201410192.

DL

Appendix A. Definition of the buckling equations

This appendix summarises the basic equations for the evaluation of the elastic buckling loads of an isolated member subjected to pure compression or to pure bending.

Column buckling loads

As well-established, the elastic critical buckling load, for a member with a non-symmetric cross-section under compression, is the minimum between the buckling loads associated with flexural, torsional and flexural-torsional modes, evaluated as follows.

Flexural buckling. Assuming y and z as the principal axes of the cross-section, the critical flexural buckling load $N_{cr,F}$ is defined as

$$N_{cr,F} = \min\left\{ N_{cr,y} = \frac{\pi^2 EI_y}{L_y^2}; N_{cr,z} = \frac{\pi^2 EI_z}{L_z^2} \right\} \quad \text{(A1)}$$

where E is the Young's modulus, I_y and I_z are the second moment of area along the principal directions and L_y and L_z are the associated effective buckling lengths.

Torsional buckling. The critical torsional buckling load $N_{cr,T}$ is defined as

$$N_{cr,T} = \frac{1}{i_0^2}\left[GI_t + \frac{\pi^2 EI_w}{L_T^2} \right] \quad \text{(A2a)}$$

with

$$i_0^2 = i_y^2 + i_z^2 + y_s^2 \quad \text{(A2b)}$$

where G is the shear modulus, I_t is the Saint Venant constant, I_w is the warping constant, i_y and i_z are the sectional radii, L_T is the torsional buckling length, y_s is the shear centre distance from the centroid of the cross-section.

Flexural-torsional buckling. It represents the combination of the previous buckling modes. For a section with y as the symmetry axis, the critical load $N_{cr,FT}$ is defined as

$$N_{cr,FT} = \frac{N_{cr,y}}{2\beta}\left[1 + \frac{N_{cr,T}}{N_{cr,y}} - \sqrt{\left(1 - \frac{N_{cr,T}}{N_{cr,y}} \right)^2 + 4(1-\beta)\frac{N_{cr,T}}{N_{cr,y}}} \right] \quad \text{(A3a)}$$

where

$$\beta = 1 - \left(\frac{y_s}{i_0} \right)^2 \quad \text{(A3b)}$$

Beam buckling moment

The elastic critical moment (M_{cr}) for a simply supported element subjected to pure bending moment, can be obtained as

$$M_{cr,B} = C_1 \frac{\pi^2 EI_z}{(k_z L)^2} \cdot \left\{ \sqrt{\left(\frac{k_z}{k_w} \right)^2 \frac{I_w}{I_z} + \frac{(k_z L)^2 GI_t}{\pi^2 EI_z} + \left(C_2 z_g + C_3 \frac{\beta_y}{2} \right)^2} - \left(C_2 z_g + C_3 \frac{\beta_y}{2} \right) \right\} \quad \text{(A4)}$$

where:

- L length of the beam between the two supports;
- E, G Young and shear moduli, respectively;
- C_1, C_2, C_3 coefficients depending on the actual distribution of the bending moment along the element (Boissonnade *et al.* 2006);
- z_g distance between the point of load application and the shear centre of the profile;
- k_z, k_w coefficients depending on the boundary condition related to the lateral displacements and warping;
- I_z second moment of area around the axis of buckling;
- I_w warping torsion constant;
- I_t Saint Venant torsion constant;
- β_y Wagner term accounting for the non-symmetry of the profiles.

The Wagner term can be evaluated as

$$\beta_y = \int z\left(z^2 + y^2\right) dA \quad \text{(A5)}$$